Analysis of fractional-order system for financial dynamics

Mateo Restrepo Sierra[1]**, Juan S. Cárdenas Rodríguez**[2]**, and David Plazas Escudero**[3]

[1]Universidad EAFIT, mrestrepos@eafit.edu.co, Student, Medellín, Colombia
[2]Universidad EAFIT, jscardenar@eafit.edu.co, Student, Medellín, Colombia
[3]Universidad EAFIT, dplazas@eafit.edu.co, Student, Medellín, Colombia

ABSTRACT

This work studies the Huang-Li financial nonlinear dynamic system, based on Chen's generalization: the given system can be also studied for non-integer order differential equations. This approach is based on two main facts that involves financial systems: chaos and memory. In one hand, it can be shown that the dynamic system in study is indeed a chaotic system; on the other hand, as financial systems are highly correlated with previous events, memory is essential, hence the use of fractional derivatives. A stability analysis and control were performed. This work is intended to give a more detailed version of the procedure mentioned in Chen's paper, since all simulation parameters for the system are specified and we include a short comparison between the numerical procedures. It was found that the system is highly controllable in both equilibrium points and periodic orbits; the stability of some points is strongly dependent on the system's order. On the other hand, a sensitivity analysis was done based on methods described on the literature and it was found that the system is sensitive to different parameters depending on the order.

Keywords: Macroeconomic financial system, fractional-order system, chaos, stability, feedback control, Adams-Bashforth-Moulton algorithm.

1 Introduction

In the study of financial systems, randomness and memory must be taken into account; thus, chaos and fractional derivatives can serve our purpose, i.e. is well known that fractional derivatives depend on the system's past and financial variables often have memory (e.g. exchange rate, interest rate, stock market prices and so on), therefore current fluctuations of variables are strongly correlated with all future fluctuations [1]. On the other hand, it is well known [2] that long-term behaviors in the financial model are highly sensitive to the initial values of the state variables and changes to the parameters (i.e. chaos). Furthermore, chaos is characterized for it's inherent randomness as it can model behaviors not available to deterministic models; in this manner, in financial systems it can help to simulate and model financial events which are indefinite. Experiments have shown that a financial system can be described by the following equations [2]:

$$\begin{aligned}
\dot{X} &= f_1(Y-\lambda)X + f_2 Z \\
\dot{Y} &= f_3(\gamma - \alpha Y - \beta X^2) \\
\dot{Z} &= -f_4 Z - f_5 X
\end{aligned} \tag{1}$$

Where X, Y and Z are the state variables that will be described in the next section and everything else are constants. The equations that are going to be worked are a particularization in China financial model of the system described above.

In this paper, we will simulate the system for different orders and compare the results with Chen's paper; a comparison between the algorithms applied for integer-order systems will be done (Runge-Kutta vs. Adams-Bashforth-Moulton), and, finally, a stability analysis and control is discussed.

2 Methodology

2.1 System Description

The system chosen for this work is taken from Chen's generalization in [1], but was originally proposed by Huang & Li in [3]. In this paper, both approaches will be studied. The dynamic system was originally proposed as a first order differential equations system, but Chen's claims this can be generalized for fractional-order differential equation system. Thus, the systems are

$$
\begin{array}{lcll}
\dot{X} = Z + (Y-a)X & & \dfrac{d^{q_1}X}{dt^{q_1}} = Z + (Y-a)X & \\
\dot{Y} = 1 - bY - X^2 & \Rightarrow & \dfrac{d^{q_2}Y}{dt^{q_2}} = 1 - bY - X^2 & q_1, q_2, q_3 \in (0,1] \\
\dot{Z} = -X - cZ & & \dfrac{d^{q_3}Z}{dt^{q_3}} = -X - cZ & \\
\textit{Original} & & \textit{Generalized} &
\end{array}
\tag{2}
$$

This financial system describes the behavior of three state variables (i.e. X, Y, Z), which are respectively the interest rate, the investment demand and the price index; a, b and c are non-negative parameters that have real interpretation, these are (respectively): savings, cost per investment, elasticity of demand. We will give a short definition for each concept:

- Interest rate (X): is the cost of borrowed money, expressed as a percentage of the loan amount [4].
- Investment demand(Y): "investment demand refers to the demand by businesses for physical capital goods and services used to maintain or expand its operations" [5].
- Price index (Z): measure of relative price changes [6].
- Savings (a): "is what a person has left over when the cost of his or her consumer expenditure is subtracted from the amount of disposable income earned in a given period of time" [7].
- Cost per investment (b): also known as pre-operative cost, it is the necessary cost that we incurred in order to start an specific project.
- Elasticity of demand (c): "measure of variable reaction to a change in another variable" If $c < 1$ is inelastic, in the other case is elastic [8].

Previous studies claim that these equations (2) were obtained through analysis and a considerable number of experiments:

- X comes from two important facts: first, the investment and savings are inversely proportional, and last the adjustment goods prices.
- Y is in proportion with the rate of investment, and in proportion to inversion with the cost of investment and the the interest rate.
- The price index Z depends on the inverse relationship between supply and demand of the commercial market; furthermore is related with the inflation rate. This is supposing that the amount of supplies and demands are constant[2].

2.2 Mathematical Model

Recall the dynamic system

$$
\begin{aligned}
\frac{d^{q_1}X}{dt^{q_1}} &= Z + (Y-a)X \\
\frac{d^{q_2}Y}{dt^{q_2}} &= 1 - bY - X^2 \\
\frac{d^{q_3}Z}{dt^{q_3}} &= -X - cZ
\end{aligned}
\tag{3}
$$

For the original approach (i.e. integer order), will be treated as a specific case of the generalized model when $q_1 = q_2 = q_3 = 1$. For the generalized model, since there are many definitions for fractional-order derivatives, the same definition as in Chen's paper will be used. Therefore, let us define the Caputo-type fractional derivative as

$$
\frac{d^\alpha y}{dx^\alpha} = D_*^\alpha y(x) = J^{m-\alpha} y^{(m)}(x), \quad \alpha > 0 \tag{4}
$$

Where $m = \lceil \alpha \rceil$ is the ceil function of α, $y^{(m)}$ is the mth ordinary derivative of y and $J^{m-\alpha}$ is the Riemann-Liouville integral operator of order $m-\alpha$. This last operator is defined as

$$J^{\beta} z(x) = \frac{1}{\Gamma(\beta)} \int_0^{\infty} (x-t)^{\beta-1} z(t) dt, \quad \beta > 0 \tag{5}$$

and $\Gamma(\beta)$ is the gamma function. For solving fractional differential equations, the Adams-Bashforth-Moulton predictor-corrector is used for numerical solutions; this method, introduced in [9], is presented in section 2.4.1.

2.3 Block Diagram

The following block diagram is only for the integer-order system with MathWork's Simulink, since the fractional order system was solved using Adams-Bashforth-Moulton predictor-corrector, in a standard Matlab script.

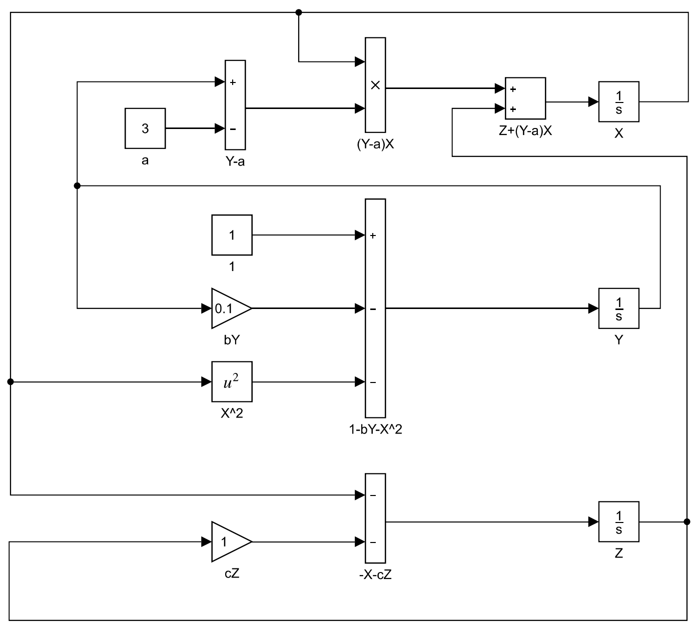

Figure 1. Block diagram for integer-order system.

2.4 Simulation Method

2.4.1 Adams-Bashforth-Moulton Algorithm

Here the pseudo-code of the algorithm will be presented as in [9], this algorithm is applied to approximate the solution of a fractional differential equation

$$D_*^{\alpha} y(x) = f(x, y(x)) \tag{6}$$

where where $\alpha > 0$ is the order of the differential equation, on a interval $[0, T]$.

INPUT VARIABLES

f = real-valued function defined for right side of the differential equation $D_*^{\alpha} y(x) = f(x, y(x))$

α = the order of the fractional differential equation, real and positive number

y_0 = array of $\lceil \alpha \rceil$ initial conditions, i.e. $y(0), y'(0), ..., y^{(\lceil \alpha \rceil - 1)}(0)$

T = positive real-valued upper limit of the approximated solution interval

N = the number of steps that the method will take in the interval

OUTPUT

$y =$ an array of $N+1$ real numbers that contains the approximation for each value of T/N in the interval

PROCEDURE

```
h = T/N
m = ⌈α⌉
for k = 1 to N do
   b[k] = k^α − (k−1)^α
   a[k] = (k+1)^(α+1) − 2k^(α+1) + (k−1)^(α+1)
end
y[0] = y0[0]
for j = 1 to N do
```

$$P = \sum_{k=0}^{m-1} \frac{(jh)^k}{k!} y_0[0] + \frac{h^\alpha}{\Gamma(\alpha+1)} \left[\sum_{k=0}^{j-1} b[j-k] f(kh, y[k]) \right]$$

$$y[j] = \sum_{k=0}^{m-1} \frac{(jh)^k}{k!} y_0[0] + \frac{h^\alpha}{\Gamma(\alpha+2)} \left[f(jh, P) + \left((j-1)^{\alpha+1} - f(0, y(0))(j-1-\alpha) j^\alpha \right) + \sum_{k=0}^{j-1} a[j-k] f(kh, y[k]) \right]$$

```
end
```

2.4.2 Runge-Kutta Method

Given the system to solve:

$$y' = f(x, y) \tag{7}$$

With the initial condition $y(0) = x_0$ and a specific time period to simulate the system h the fourth order Runge-Kutta method dictates that the solution:

$$y_{i+1} = y_i + \frac{h}{6}(k_1 + 2k_2 + 2k_3 + k_4) \tag{8}$$

With:

$$\begin{aligned}
k_1 &= f(x_i, y_i) \\
k_2 &= f(x_i + \tfrac{h}{2}, y_i + \tfrac{hk_1}{2}) \\
k_3 &= f(x_i + \tfrac{h}{2}, y_i + \tfrac{hk_2}{2}) \\
k_4 &= f(x_i + \tfrac{h}{2}, y_i + hk_3)
\end{aligned} \tag{9}$$

Furthermore, this method has different versions due to the application of different orders of this algorithm [10]; therefore, it would be expected that this method is more precise than the Adam-Bashforth-Moulton because is three orders less compared to Runge-Kutta when both used to solve integer derivatives. On the other hand, there is no way to use the first method to solve fractional derivatives in higher orders (at least with reasonable complexities) therefore the Adam's algorithm has more computability than the Kutta's. This method was used for the specific case for integer-order model i.e. $q_1 = q_2 = q_3 = 1$.

3 Results & Discussion

For all of the following simulations, we set the value of the parameters to $a = 3$, $b = 0.1$ and $c = 1$ with the initial condition of $(X_0, Y_0, Z_0) = (2, 3, 2)$. As the numerical method used to solve the fractional-order equations needs a certain time of simulation (T) and number of iterations (N) it was used $N = 10000$ and $T = 1000$ thus the time-step is 0.1. It is important to highlight, that the results of the simulation are strongly dependent of the value of the last conditions to obtain the same result as the presented in this article.

3.1 Comparison between Chen's paper and results obtained

3.1.1 Equal fractional order system

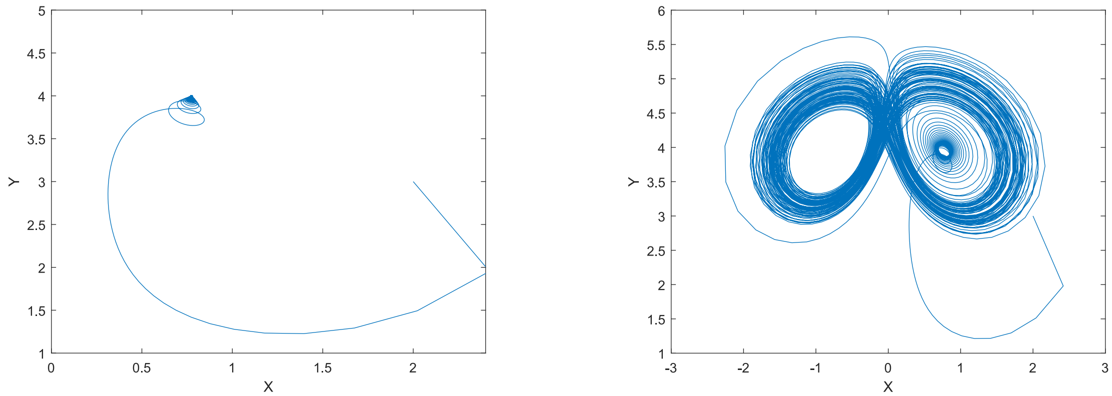

(a) Results when $\alpha = 0.84$. **(b)** Results when $\alpha = 0.85$.

Figure 2. Results for equal fractional order system when $q_1 = q_2 = q_3 = \alpha$.

In figure 2, the results for equal fractional order are shown. These plots are comparable with the ones showed in Chen's paper [1] in figure 2 (a-b). On the figure 2a, it can be observed that the plots are slightly different. On the other hand, on figure 2b the shape is highly similar to the original but, the filling of the graph is not comparable. It would be explained later why this dissimilarities occur. Note that the system changes from a stable trajectory to a chaotic one with a small change on the order. This result will be discussed in the stability analysis section.

3.1.2 Non-equal fractional order systems

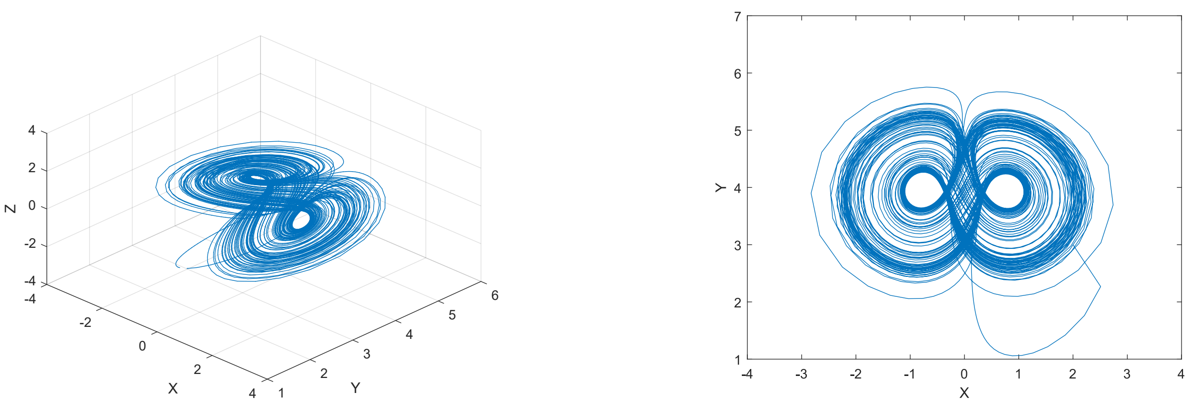

(a) $q_1 = 0.90$ **(b)** $q_1 = 0.80$

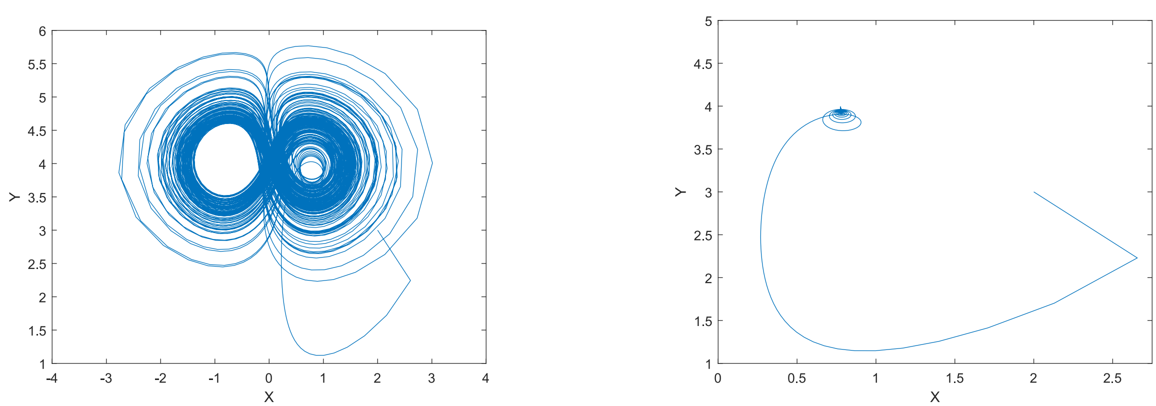

(c) $q_1 = 0.70$ **(d)** $q_1 = 0.65$

Figure 3. Results for $q_2 = q_3 = 1$

In figure, 3a it was shown the third-dimensional graph instead of a phase-state plane just for illustration purposes. On the remaining it can be seen their similitude with Chen's article.

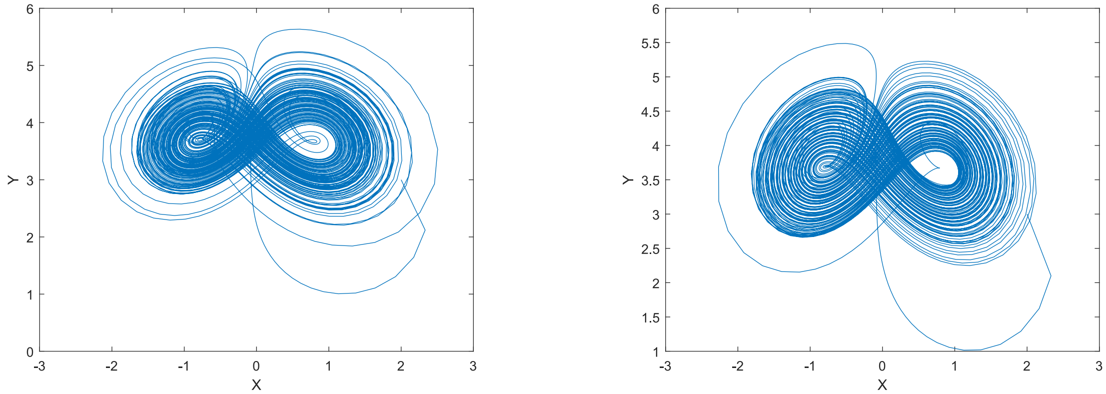

(a) $q_2 = 0.90$. **(b)** $q_2 = 0.89$.

Figure 4. Results for $q_1 = q_3 = 1$.

Figures 4(a-b) are matched to the Figures 3(c-d) in Chen's paper. It can be seen that both graphics are quite different to the ones presented at the original article. Figure 4b graphic has the most considerable difference; even though, it preserves the uniformity of the graph.

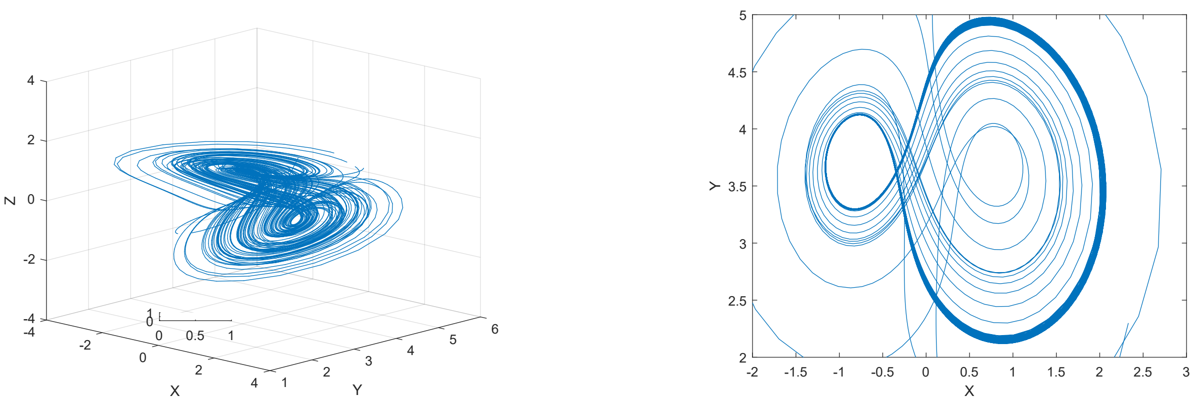

(a) $q_3 = 0.90$ **(b)** $q_3 = 0.80$

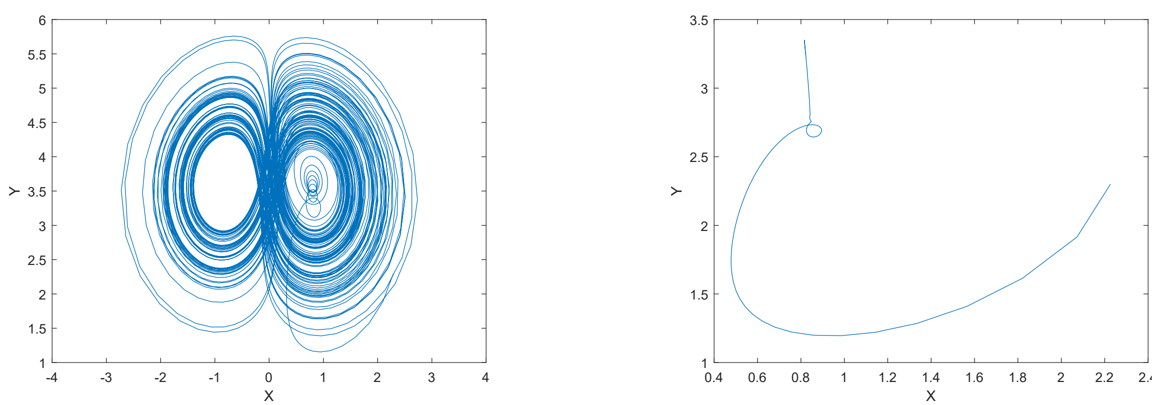

(c) $q_3 = 0.70$ **(d)** $q_3 = 0.20$

Figure 5. Results for $q_1 = q_2 = 1$

All of the figures depicted at Figure 5 are associated to the 5th Figure of Chen. It can be perceived that all of the plots shown above are interchangeable one another with the exception of Figure 5b. But, the chart mentioned preserves the shape of the primal.

The differences of the above phase-state portraits could be explained by a number of causes. First of all, Chen does not specifies the time-step nor the upper-bound of the time interval about the simulation that they run; therefore, the lines in the plots can have more iterations thus have more trajectories. On the other hand, Figures 2a, 3d or 5d as they converge to one specific point, it is not as dependent of the time iterations as the rest, therefore their similitude with the original is almost perfect. Another cause for this difference is that the modifications for the Adams-Bashforth-Moulton predictor-corrector, recommended in [9], were not applied for the simulations. It is important to highlight that small changes on the system's order lead to big changes on its behavior.

3.2 Comparison between Runge-Kutta method and Adams-Bashforth-Moulton predictor-corrector

In this section, it will be compared the results that both methods give using integer order differentiation. The parameters $a = b = c = 0$ were used, therefore the figure 6 can be compared to the second figure of article [11]. In the figure 6 the initial conditions were $(x_0, y_0, z_0) = (0, 0, 2.21)$ and for the next ones, $(x_0, y_0, z_0) = (0, 0, 1.6)$ was used.

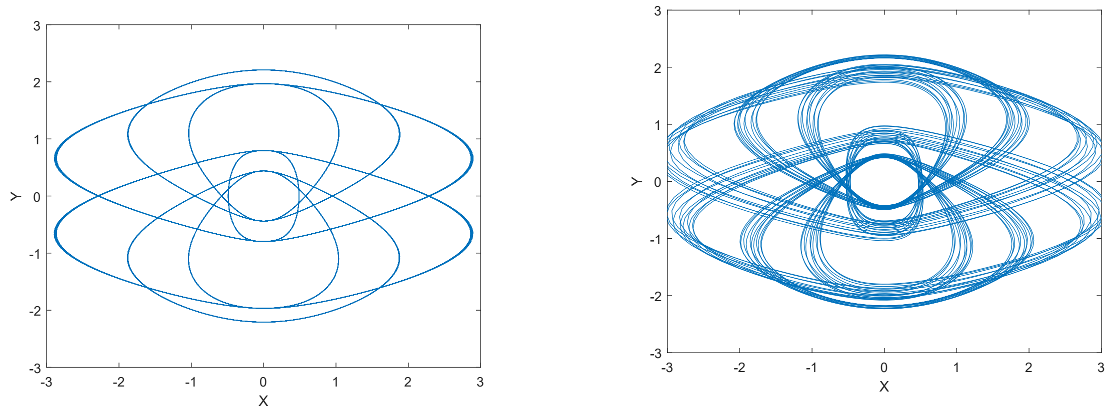

(a) Results using Runge-Kutta method.

(b) Results using Adams-Bashforth-Moulton predictor-corrector.

Figure 6. Results for integer-order system, i.e. $q_1 = q_2 = q_3 = 1$

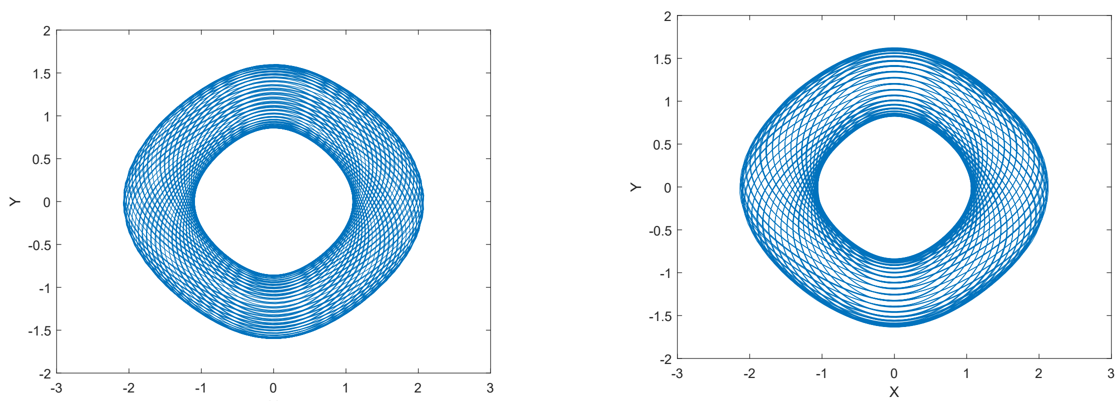

(a) Results using Runge-Kutta method.

(b) Results using Adams-Bashforth-Moulton predictor-corrector.

Figure 7. Results for integer-order system, i.e. $q_1 = q_2 = q_3 = 1$

It can be shown that both graphs keep the same form independently of the method used; as explained before, the Runge-Kutta is more precise than the other numerical method due to the difference of order. Therefore, every discrepancy of the plots can be explained with the above.

4 Stability Analysis

4.1 Preliminaries

For the stability analysis of the fractional order system, the following theorem and definition, proposed and proved in [12], were applied:

Definition 1. Given a nonlinear differential system

$$_{C}D^{p}_{0,t}x(t) = f(x(t)), \quad x(t) \in \mathbb{R}^{n} \tag{10}$$

where $x(0) = x_0$, $f(x)$ is continuous, the point e is an equilibrium point of this system, if and only if $f(e) = 0$.

Theorem 1. *Let $x = x^*$ be an equilibrium point of a fractional nonlinear system*

$$D^{\alpha}x = f(x), \quad 0 < \alpha < 2 \tag{11}$$

If the eigenvalues of the Jacobian matrix $A = \partial f/\partial x|_{x=x^*}$ satisfy

$$\min_i |\arg(\lambda_i)| > \alpha\frac{\pi}{2}, \quad i = 1, 2, \ldots, n. \tag{12}$$

then x^* is asymptotically stable.

4.2 Results

Analyzing the system shown in 2 and applying the definition 1, the equilibrium points are:

$$\begin{aligned} &p_1: \quad X = 0 \quad Y = \frac{1}{b} \quad Z = 0 \\ &p_{2,3}: X = \pm\sqrt{\frac{c - b - abc}{c}} \quad Y = \frac{1 - x^2}{b} \quad Z = -\frac{x}{c} \end{aligned} \tag{13}$$

Now, to analyze the stability of these equilibrium points, the Jacobian of the state variables is needed, thus

$$J = \begin{bmatrix} Y - a & X & 1 \\ -2X & -b & 0 \\ -1 & 0 & c \end{bmatrix} \tag{14}$$

For the following simulations, the values for a, b and c will be, respectively, 3, 0.1 and 1; $q_1 = q_2 = q_3 = \alpha$ and $0 < \alpha < 1$ is assumed as well. Therefore, to use theorem 1, the eigenvalues of the Jacobian matrix are required; using p_1 and $p_{2,3}$ as analysis points, the stability will be determined:

With the given values, $p_1 = (0, 10, 0)$ and then respective Jacobian matrix is

$$J_{p_1} = \begin{bmatrix} 7 & 0 & 1 \\ 0 & -0.1 & 0 \\ -1 & 0 & -1 \end{bmatrix} \tag{15}$$

with eigenvalues $\lambda_1 = -0.1$, $\lambda_2 \approx 6.8730$ and $\lambda_3 \approx -0.8730$. Now, theorem 1 is applied, $\min|\arg(\lambda_1), \arg(\lambda_2), \arg(\lambda_3)| = \min|\pi, \pi, 0| = 0 < \alpha\frac{\pi}{2}$ since $0 < \alpha < 1$; therefore, according to the theorem, p_1 is an unstable equilibrium point.

Following a similar procedure for $p_{2,3}$, it can be obtained that the eigenvalues are $\lambda_1 \approx -0.7256$, $\lambda_2 \approx 0.3128 - 1.2474i$ and $\lambda_3 \approx 0.3128 + 1.2474i$. In this case, we shall analyze the order of the fractional differential equation system (α). Given

$$\min_i |\arg(\lambda_i)| > \alpha\frac{\pi}{2}$$

It can solved for α and obtain a critical value for the order, hence

$$\alpha < \frac{2}{\pi}\min_i |\arg(\lambda_i)| \tag{16}$$

In this case, $\alpha < \frac{2}{\pi}\min_i|\arg(\lambda_1), \arg(\lambda_2), \arg(\lambda_3)| = \frac{2}{\pi}(1.3251) \approx 0.8436$. Therefore, if $\alpha < 0.8436$ the point $p_{2,3}$ is asymptotically stable; in any other case, is unstable.

5 Control

5.1 Preliminaries

It is desired to stabilize the system 2 in a periodic orbit (or in a fixed point) $(\tilde{x}, \tilde{y}, \tilde{z})$ using feedback control, as in [12], hence

$$\begin{aligned} \frac{d^{q_1}X}{dt^{q_1}} &= Z + (Y-a)X + u_1(t) \\ \frac{d^{q_2}Y}{dt^{q_2}} &= 1 - bY - X^2 + u_2(t) \\ \frac{d^{q_3}Z}{dt^{q_3}} &= -X - cZ + u_3(t) \end{aligned} \tag{17}$$

Following the procedure described in [12], the control functions are defined by

$$\begin{aligned} u_1(t) &= -(xy - \tilde{x}\tilde{y}) \\ u_2(t) &= x^2 - \tilde{x}^2 \\ u_3(t) &= x - \tilde{x} \end{aligned} \tag{18}$$

5.2 Results

5.2.1 Stabilizing the system to a periodic orbit

For the following simulations, $\alpha = 0.9$ will be used. Additionally, the same values from section 4 for a, b and c are used. The solution to the system was obtained with the same Adams-Bashforth-Moulton predictor-corrector, with $N = 3000$ and $T = 300$.

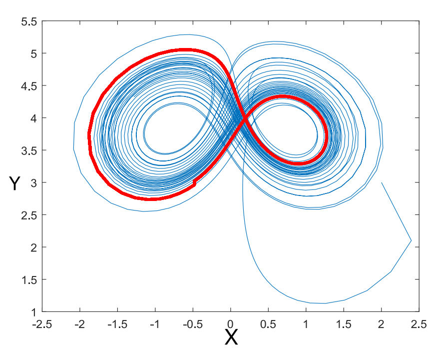

(a) Uncontrolled phase plane for XY with selected orbit.

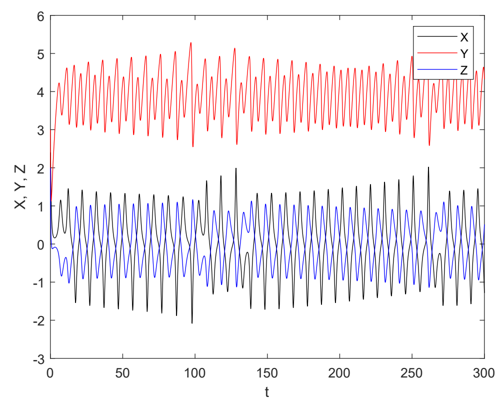

(b) Uncontrolled XYZ against time.

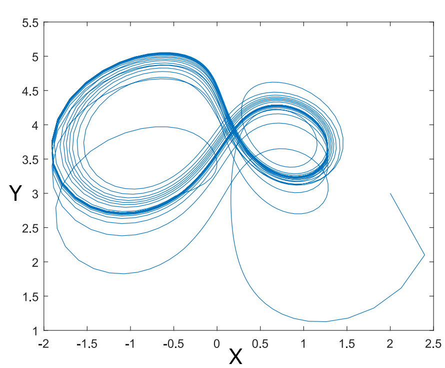

(c) Controlled phase plane for XY.

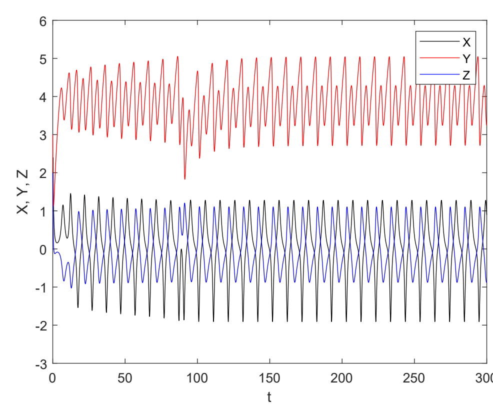

(d) Controlled XYZ against time.

Figure 8. Results for controlled system in the selected orbit.

In figure 8a, the red path is the selected periodic orbit to stabilize. The period of said orbit is 10.2, the interval for it is $[78.2, 88.4]$. On figure 8b, the behavior of the state variables through time is shown, note the periodic behavior of these variables through time after the control is applied.

In figure 8(a-b), the response for the proposed control is shown. The controller starts when the system fully completes the selected orbit (i.e $t = 88.4$), in order to ensure that it remains in a similar shape. Before applying the feedback control, $u_i(t) = 0$, $i = 1,2,3$. Note that the response is periodic and more consistent compared to the original.

5.2.2 Stabilizing the system to a fixed point

In this section, the same α, a, b and c are used as in the previous simulations, except for the last plot (i.e figure 10) that $\alpha = 0.95$. In order to obtain these results, the controller starts working at $t = 22.5$.

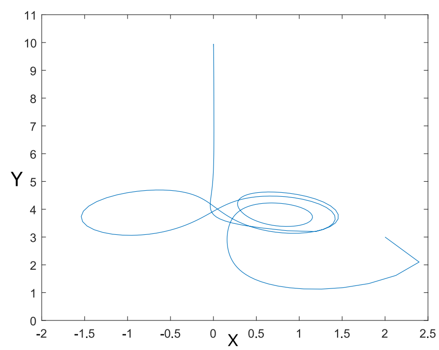

(a) Phase plane for XY.

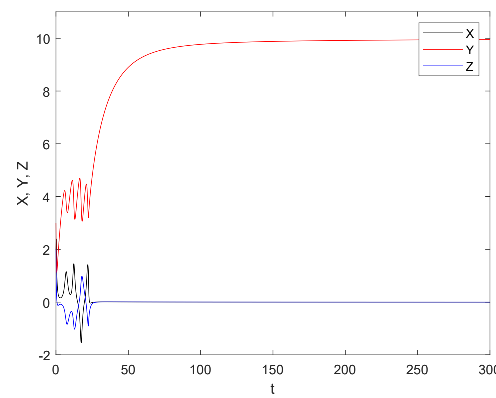

(b) XYZ against time.

Figure 9. Results for controlled system around p_1.

In figure 9, the stabilization for the equilibrium point $p_1 = (0, 10, 0)$ is exhibited. The figure on the left shows how the system converges to this point. The figure on the right shows the behavior of the states variables through time, showing that they also converge to p_1.

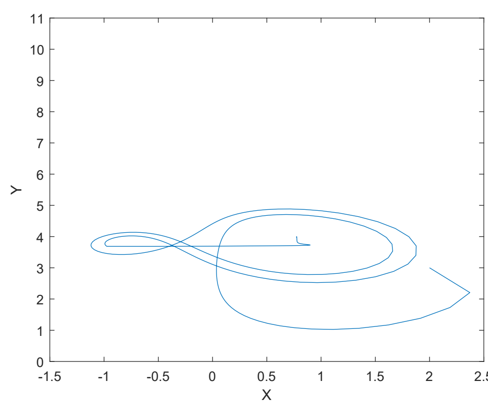

(a) Phase plane for XY.

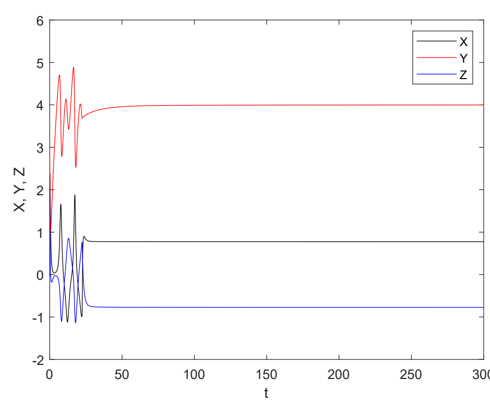

(b) XYZ against time.

Figure 10. Results for controlled system around p_2.

In figures 10(a-b), the equilibrium is achieved around p_2, using the same procedure as in the previous simulation. Note that $\alpha = 0.95$.

The results obtained in this section can be compared with fixed-point stabilization in Abd-Elouahab *et al.* in [12].

It can be seen that the system is highly controllable, through the feedback control methodology presented in [12]. There are others types of controllers proposed in the literature for this fractional-order system; see [13] or [14].

6 Sensitivity Analysis

Recall the fractional dynamic system that is being studied

$$\begin{aligned}
\frac{d^{\alpha}X}{dt^{\alpha}} &= Z+(Y-a)X \\
\frac{d^{\alpha}Y}{dt^{\alpha}} &= 1-bY-X^2 \qquad \alpha\in(0,1] \\
\frac{d^{\alpha}Z}{dt^{\alpha}} &= -X-cZ
\end{aligned} \tag{19}$$

The main goal is measure the sensibility of parameters a, b and c as in [15].

For our first simulation, we will be analyzing the commensurate system (i.e same derivative order), $\alpha = 0.84$ will be used. The initial values for the parameters are (μ_0): $a_0 = 3$, $b_0 = 0.1$ and $c_0 = 1$. In order to calculate the behavior of X, Y and Z respect to a, b and c, the associated Jacobian matrices are required. Let x be the vector of the state variables and μ the vector of parameters; hence,

$$P(t,\mu_0) = \frac{\partial f}{\partial x}\Big|_{\mu_0} = \begin{bmatrix} Y-3 & X & 1 \\ -2X & -0.1 & 0 \\ -1 & 0 & 1 \end{bmatrix} \qquad Q(t,\mu_0) = \frac{\partial f}{\partial \mu}\Big|_{\mu_0} = \begin{bmatrix} -X & 0 & 0 \\ 0 & -Y & 0 \\ 0 & 0 & -Z \end{bmatrix} \tag{20}$$

Let the sensitivity function

$$S(t) = \frac{\partial f}{\partial x}\Big|_{\mu_0} = \begin{bmatrix} \frac{\partial X}{\partial a} & \frac{\partial X}{\partial b} & \frac{\partial X}{\partial c} \\ \frac{\partial Y}{\partial a} & \frac{\partial Y}{\partial b} & \frac{\partial Y}{\partial c} \\ \frac{\partial Z}{\partial a} & \frac{\partial Z}{\partial b} & \frac{\partial Z}{\partial c} \end{bmatrix} \triangleq \begin{bmatrix} X_a & X_b & X_c \\ Y_a & Y_b & Y_c \\ Z_a & Z_b & Z_c \end{bmatrix} \tag{21}$$

Where $S(t)$ contains the new state variables for our system. These variables measure how the state variables change respect to the parameters. Now, the sensitivity equation is defined as

$$\begin{aligned}
\frac{d^{0.84}S(t)}{dt^{0.84}} &= P(t,\mu_0)S(t)+Q(t,\mu_0) \\
&= \begin{bmatrix} Y-3 & X & 1 \\ -2X & -0.1 & 0 \\ -1 & 0 & 1 \end{bmatrix} \begin{bmatrix} X_a & X_b & X_c \\ Y_a & Y_b & Y_c \\ Z_a & Z_b & Z_c \end{bmatrix} + \begin{bmatrix} -X & 0 & 0 \\ 0 & -Y & 0 \\ 0 & 0 & -Z \end{bmatrix}
\end{aligned} \tag{22}$$

Now, combining the original system and the sensitivity equation, we obtain the new fractional dynamic system

$$
\begin{cases}
\dfrac{d^\alpha X}{dt^\alpha} = Z + (Y-3)X, & X(0) = X_0 \\
\dfrac{d^\alpha Y}{dt^\alpha} = 1 - 0.1Y - X^2 & Y(0) = Y_0 \\
\dfrac{d^\alpha Z}{dt^\alpha} = -X - Z & Z(0) = Z_0 \\
\dfrac{d^\alpha X_a}{dt^\alpha} = Z_a - (1+Y_a)X - (3-Y)X_a & X_a(0) = 0 \\
\dfrac{d^\alpha X_b}{dt^\alpha} = Z_b + XY_b - (3-Y)X_b & X_b(0) = 0 \\
\dfrac{d^\alpha X_c}{dt^\alpha} = Z_c + XY_c - (3-Y)X_c & X_c(0) = 0 \\
\dfrac{d^\alpha Y_a}{dt^\alpha} = -0.1Y_a - 2XX_a & Y_a(0) = 0 \\
\dfrac{d^\alpha Y_b}{dt^\alpha} = -Y - 0.1Y_b - 2XX_b & Y_b(0) = 0 \\
\dfrac{d^\alpha Y_b}{dt^\alpha} = -0.1Y_c - 2XX_c & Y_b(0) = 0 \\
\dfrac{d^\alpha Z_a}{dt^\alpha} = -X_a - Z_a & Z_a(0) = 0 \\
\dfrac{d^\alpha Z_b}{dt^\alpha} = -X_b - Z_b & Z_b(0) = 0 \\
\dfrac{d^\alpha Z_c}{dt^\alpha} = -Z - X_c - Z_c & Z_c(0) = 0
\end{cases}
\tag{23}
$$

Adams-Bashforth-Moulton predictor-corrector with $T = 1000$, $N = 10000$ and $(X_0, Y_0, Z_0) = (2, 3, 2)$ was used.

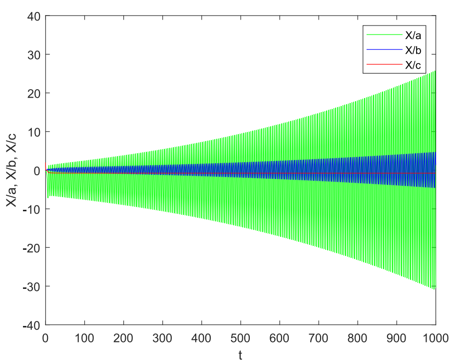

(a) Change of X.

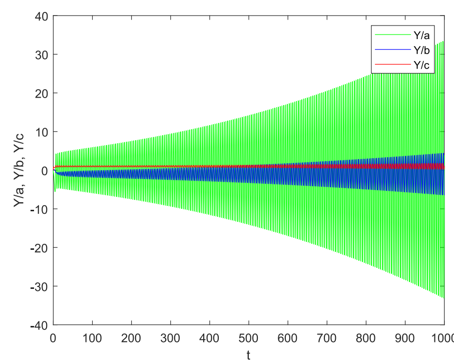

(b) Change of Y.

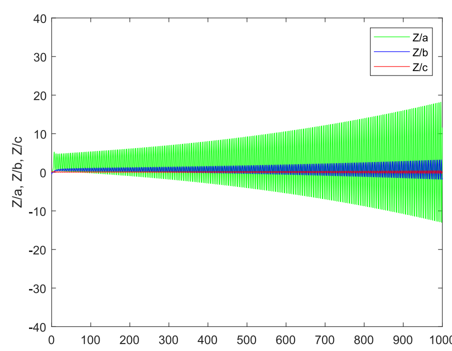

(c) Change of Z.

Figure 11. Changes of state variables respect to parameters.

In figure 11, the results for the sensitivity can be observed for $\alpha = 0.84$. Note that, for all state variables, its change respect to a is predominant over b and c.

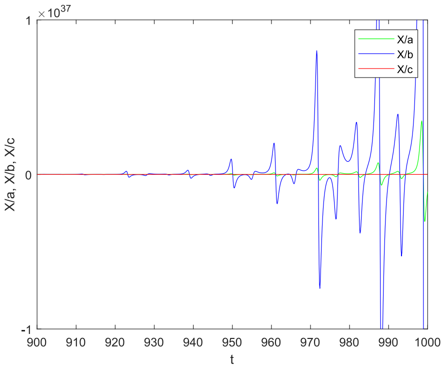

(a) Change of X.

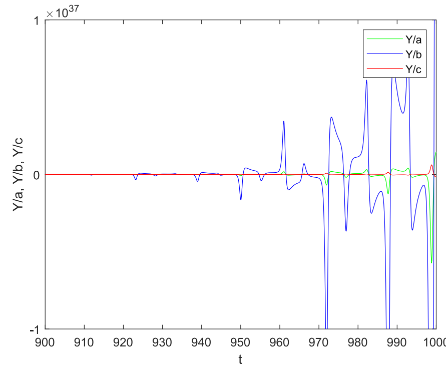

(b) Change of Y.

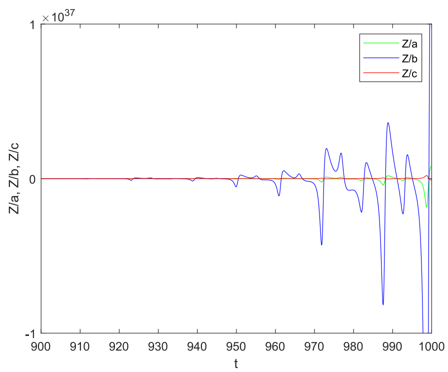

(c) Change of Z.

Figure 12. Changes of state variables respect to parameters.

In figure 12, the results for the sensitivity can be observed for $\alpha = 0.85$. Note that, for all state variables, its change respect to b is predominant over a and c. Remark: the previous simulation was made with the same $T = 1000$ and $N = 10000$ as in the one with $\alpha = 0.84$, but the plot was made only between $900 \leq t \leq 1000$ for a better visualization of system's behavior.

Comparing the results for $\alpha = 0.84$ and $\alpha = 0.85$, it can be concluded that, in the first simulation, the system is not as sensitive as the one in the second simulation, since the rate of change for b is in the order of 10^{37} and for a in the first one is in the order of 10^1.

In figure 2a, it can be seen the phase diagram for $\alpha = 0.84$ and in section 4 it was proved that this system converges to a stable equilibrium point and the sensitivity analysis showed a bounded non-decreasing periodic behavior.

In figure 2b, it can be observed the phase diagram for $\alpha = 0.85$ and in section 4 it was proved that this system has unstable equilibrium points and the sensitivity analysis showed a random oscillation, like a noise signal.

This suggests that there could be a relation between the stability of the system and its sensitivity.

7 Conclusions

It can be concluded that the graphs coincide in this paper and the Chen's paper using the Adams-Bashforth-Moulton predictor-corrector. Each discrepancy are due to the time-step and the interval of simulation; we suggest that in further work this is more clear so that the results are easier to replicate. In second place, we found that Adams' method can be, to a certain extent, equivalent to the Runge-Kutta method; taking into account, that the orders of both algorithms are different the similitude is a very good approximation. It was also shown that the generalized equations conserve the properties of memory and randomness that are fully necessary to simulate the macro-financial system of China.

On the other hand, it was seen that the system has three equilibrium points: one of them (p_1) will always be unstable, and the other ones (p_2, p_3) depend on the system's order (α). Additionally, it was found that the system has a critical value for $\alpha = 0.8436$, which is when the stability changes.

A successful control for both equilibrium points and periodic orbits was achieved; showing that the system, regardless of its chaotic behavior, can be stabilized.

Finally, a sensitivity analysis was developed successfully, based on the methods described on literature; based on this results, it could be observed that the sensitivity is highly dependent on the order of the system, yielding different results for each order.

In future work, it could be analyzed the sensitivity for the incommensurate system; furthermore, the system could be analyzed for $\alpha > 1$, verifying if the Adams-Bashforth-Moulton predictor-corrector converges for these orders and developing a methodology for both control and sensitivity.

References

[1] W.-C. Chen, "Nonlinear dynamics and chaos in a fractional-order financial system," *Chaos, Solitons & Fractals*, vol. 36, no. 5, pp. 1305–1314, 2008.

[2] M. Jun-hai and C. Yu-Shu, "Study for the bifurcation topological structure and the global complicated character of a kind of nonlinear finance system (i)," *Applied Mathematics and Mechanics*, vol. 22, no. 11, pp. 1240–1251, 2001.

[3] D. Huang and H. Li, "Theory and method of the nonlinear economics," *Publishing House of Sichuan University, Chengdu*, 1993.

[4] Investopedia, "Interest rate," 2018, accessed 2018-09-26. [Online]. Available: https://www.investopedia.com/terms/i/interestrate.asp

[5] S. Suranovic, *Policy and Theory of International Finance*, 2012. [Online]. Available: https://2012books.lardbucket.org/books/policy-and-theory-of-international-finance/s11-04-investment-demand.html

[6] T. E. of Encyclopaedia Britannica, "Price index," 2014, accessed 2018-09-27. [Online]. Available: https://www.britannica.com/topic/price-index

[7] Investopedia, "Savings," 2018, accessed 2018-09-26. [Online]. Available: https://www.investopedia.com/terms/s/savings.asp

[8] Investopedia2, "Demand elasticity," 2018, accessed 2018-09-26. [Online]. Available: https://www.investopedia.com/terms/d/demand-elasticity.asp

[9] K. Diethelm, N. J. Ford, and A. D. Freed, "A predictor-corrector approach for the numerical solution of fractional differential equations," *Nonlinear Dynamics*, vol. 29, no. 1-4, pp. 3–22, 2002.

[10] J. Kiusalaas, *Numerical methods in engineering with python 3*. Cambridge University Press, 2013.

[11] W. Szuminski, "Non-integrability of huang-li nonlinear financial model," *Institute of Physics, University of Zielona Gora*, 2017.

[12] M. S. Abd-Elouahab, N.-E. Hamri, and J. Wang, "Chaos control of a fractional-order financial system," *Mathematical Problems in Engineering*, vol. 2010, 2010.

[13] I. Pan, S. Das, and S. Das, "Multi-objective active control policy design for commensurate and incommensurate fractional order chaotic financial systems," *Applied Mathematical Modelling*, vol. 39, no. 2, pp. 500–514, 2015.

[14] Y. Yang and G. Cao, "Modified function projective synchronization for a partially linear and fractional-order financial chaotic system with uncertain parameters," *Discrete Dynamics in Nature and Society*, vol. 2017, 2017.

[15] Y. Guo, B. Ma, and R. Wu, "On sensitivity analysis of parameters for fractional differential equations with caputo derivatives," *Electronic Journal of Qualitative Theory of Differential Equations*, vol. 2016, no. 118, pp. 1–17, 2016.